Magnetic Field Shielding for the Forward Time of Flight Upgrade at Jefferson National Lab

By

Robert Steinman

Bachelor of Science

Indiana University of Pennsylvania, 2008

Submitted in Partial Fulfillment of the Requirements

for the Degree of Master of Science in Physics

College of Arts and Sciences

University of South Carolina

2010

Dr. Ralf Gothe, Director of Thesis

Dr. Milind Purohit, Reader

Dr. Yordanka Ilieva, Reader

Dr. Jim Buggy, Dean of the Graduate School

UMI Number: 1475741

UMI®

Dissertation Publishing

ProQuest®

For my mom who was always behind me, my father who was always beside me, and my sister who was always in front of me.

-Robbie

Acknowledgements

I honestly would not have made it this far if Dr. Ralf Gothe had not been there for me when I was drowning in the sea of physics knowledge. His guidance, support, and gentle prodding has helped me to grow more in two years of graduate school than I ever thought possible.

To Evan Phelps, I thank you for listening to my complaints about all matters of things, and for helping me to better understand physics when you could have probably been working on your own material.

To Ye Tian, you are the embodiment of a hard working student and put most of us in the group to shame. I hope you feel very good about yourself, because you certainly should.

To Eric Graham, thank you for never giving me just the answer and forcing me to work the problems for myself. I only now realize what you were trying to do for me.

And finally, Lewis Graham, Haiyun Lu, and Zhiwen Zhao provide the light at the end of the very…very…long graduate tunnel.

Abstract

The University of South Carolina has been tasked with the construction of the counters for the Forward Time of Flight detector during Jefferson Lab's 12-GeV upgrade. The counters, consisting of photomultiplier tubes attached to the ends of scintillation bars of varying lengths, record the time of flight for particles inside the Continuous Electron Beam Accelerator Facility (CEBAF) Large Acceptance Spectrometer (CLAS). These detectors must be properly shielded from magnetic fields used in the manipulation of the particle trajectories during experiments. Dr. Gothe's nuclear physics group has been experimenting with various types of magnetic shielding methods using a Helmholtz Coil to provide varying field strengths. Photomultiplier tubes with magnetic shielding built in supply the necessary shielding for the strengths expected at Jefferson Lab, though there are still other options available if need be.

Table of Contents

List of Figures

I.   An Introduction to the CLAS 12-GeV Upgrade

The amount of knowledge humans have about the world has always been linked to the level of technology available during the time. It would have been rather simple for Galileo to prove that the Earth was round if given access to the Hubble Space Telescope. It took the postulates of Albert Einstein decades to be verified with modern technology. We as a species learn more about the world around us through the use of technology. With that in mind, we must always push technology to the breaking point to expand our level of knowledge.

This mentality, along with the desire to learn more about the strong force and nuclei, is leading the way for construction at Jefferson National Lab. Scattering experiments have proven invaluable in increasing our level of understanding about atoms, the protons and neutrons that make up the nucleus, along with their own constituents the quarks and gluons. But the current 6-GeV electron beam can only provide us with so much information. A higher energy and higher luminosity beam allows for advanced studies in the structure of the nucleons and nuclei. (Graham, 2008)

Jefferson Lab houses CEBAF, the Continuous Electron Beam Accelerator Facility, where the CLAS detector is currently undergoing a massive upgrade to 12-GeV. This will involve the upgrade of the current Forward Detector and construction of a new Central Detector around the target area.
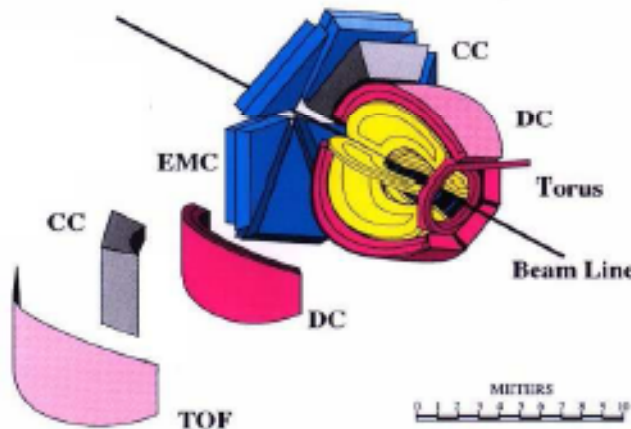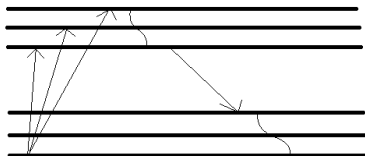
Forward Detector

The Forward Detector is the main focus of the 12-GeV upgrade work done at the University of South Carolina. A torus magnet inside CLAS provides an azimuthally symmetric magnetic field (CLAS12 Technical Design Report v5.0, 2008), allowing the manipulation of the particle's trajectory inside the detector. Drift Chambers detect the trajectories of the particles, while the Cherenkov Counters discriminate electrons from all the other particles in the desired reactions. Scintillation Counters measure the time of flight of particles from the target to the detector. These counters consist of scintillation material and photomultiplier tubes. Electromagnetic Calorimeters detect showering particles. Data from the detector is acquired through a two-level trigger system. The Data Acquisition collects all digitized data from the detector and stores it for later analysis. USC is currently in charge of providing the optimum time resolution for the Time of Flight (TOF) detectors to accurately identify particles inside the detector. (Graham, 2008)

II.   Scintillation Material

Scintillation material is used in the TOF detector because of its unique

properties. An incident particle passing through the scintillation material creates

excited states, and returning to the ground states requires the emission of photons.

These photons could be reabsorbed by other atoms in the material, preventing the

photon from ever reaching the photocathode of the photomultiplier tube, but a unique

characteristic of scintillation material prevents this from occurring. The excited and

ground states of the scintillator feature vibrational bands, or small discrepancies in

these states. Phonon emissions within the bands reduce the energy of the excited

states. To reach its ground state, the scintillation material emits a photon that typically

does not have the same amount of energy from the excitation anymore, because of the

reduction through the vibrational bands. This prevents the photons from exciting

ground state electrons again, allowing the photon to travel through the scintillator to

the photocathode. On the ends of each scintillation detector are photomultiplier tubes,

which convert the light into a current proportional to the number of photons collected.

illation material.

III.   Photomultiplier Tubes

The photomultiplier tubes (PMTs) are used to convert light from the scintillation material into a measurable electric current. The tube itself consists of a photocathode made of photosensitive material, an electron collection system, and an electron multiplier section. The entire structure is encased in an evacuated tube.

Photocathode

The photocathode converts light into a current of electrons via the photoelectric effect. A thin layer of photosensitive material is deposited on the inside of the PMT window. The kinetic energy of the emitted electron can be found using

$$E = h\nu - \phi,$$

where h is Planck's Constant, ν is the frequency of the incident light and ϕ is the work function of the material.   A minimum frequency is required for the photoelectric effect to take effect. To determine the conversion efficiency of the PMT, it is necessary to relate the number of emitted photoelectrons $N_{\gamma e}$ to the number of incident photons N_γ on the surface of the photoelectric material.

$$\eta(\lambda) = \frac{N_{\gamma e}}{N_\gamma}$$

This quantum efficiency of the material, that depends on the wavelength of the incident light λ, is important in choosing which material to use for the photocathode. Semi-conducting materials are commonly used because the quantum efficiency of 10%-30% is high when compared to 0.1% for various metals.

The Electron-Optical Input System

The electrons emitted by the photocathode must be focused onto the first dynode of the signal-amplification process. This is usually done using a focusing electric field inside of the PMT. The process must be as efficient as possible, meaning as many photoelectrons as possible must reach the electron-multiplier section of the PMT, regardless of where they are emitted on the photocathode. The time it takes to reach the first dynode must also be as independent as possible from the point of emission on the cathode. This is necessary to prevent any detrimental transition-time jitter on time resolution measurements.

The Electron-Multiplier Section

The photoelectrons leaving the photocathode carry very little energy. A series of dynodes (typically 10 to 14) are arranged in a ladder-type pattern that emits secondary electrons upon each interaction with the incoming electrons. The typical gain through the PMT is 3×10^7 for the number of electrons converted through the photocathode. The amplified signal leads directly into the anode at the end of the PMT, which can then be read for analysis.

IV.   Photomultiplier Tubes in a Magnetic Field

In the presence of a magnetic field, the analog signal coming from the PMT can be reduced, depending on the strength and geometry of the field (Armstrong & Smith, 1991). This is due to the electrons within the tube experiencing a Lorentz Force on their way to the anode output,

$$\vec{F} = q \ (\vec{v} \ \times \vec{B}),$$

where q is the charge of the electrons. Obviously, the intensity of the magnetic field directly determines how much force the electrons will feel, but the geometry of the field is also of great importance to the amplitude reduction. Electrons inside the PMT are deflected, which can lead to signal reduction. Two distinct magnetic field configurations were considered during the initial analysis[1]: an axial field and a transverse field as illustrated in Figure 3. The axial field is incident on the photocathode end of the PMT, while the transverse field acts perpendicular to the side casing. A uniform magnetic field created inside of a Helmholtz Coil acts as an analog to the fields inside of the CLAS12 detector at Jefferson National Lab. To study the effects of a magnetic field on the PMT output, a single PMT detector is placed inside of the coil to output data under varying magnetic fields strengths and orientations.

---

[1] See Amplitude and Signal-Shape Test Using an Oscilloscope on pg. 9.

Transverse   Axial
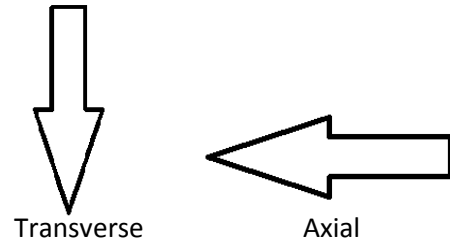
Figure 3: Fully constructed PMT detector.

Magnetic Field Calibration

Because this test is to be repeated many times with different PMTs and

geometries, a magnetic field calibration for the Helmholtz Coil is needed. The current

running through the coils is directly compared to the amount of magnetic field produced

in the center of the two coils (where the field is most uniform). Figure 4 shows the

Helmholtz Coil used in the experiment, while Figure 5 shows the magnetic field

calibration. A Gauss Meter measures the magnetic field due to various currents for

proper calibration. The Helmholtz Coil is set to the desired magnetic field strength for

fifteen minutes to allow for uniform and repeatable conditions. This warm up period is

crucial to maintain the magnetic field at a constant value during the experiment. The

current is supplied by a DC power source featuring a digital current readout. An

ammeter connected to the Helmholtz Coil verifies the digital readout on the current

source.
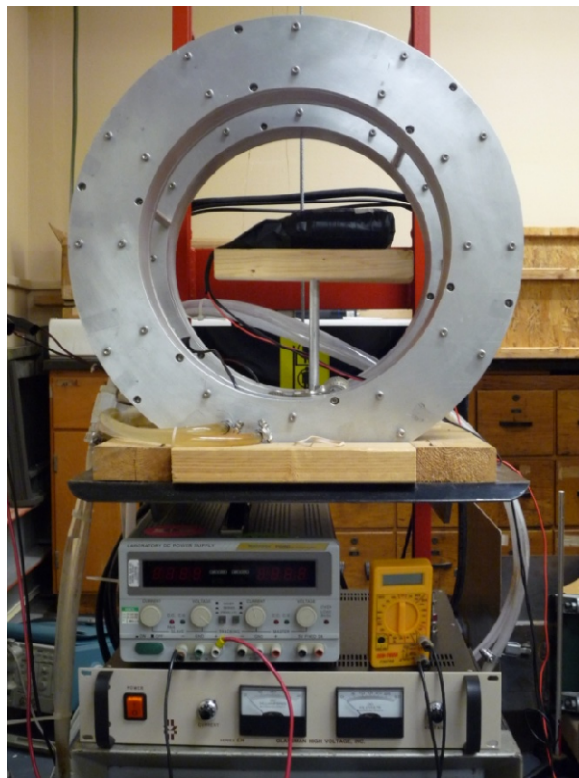
Figure 4: Helmholtz Coil w/ detector stand.
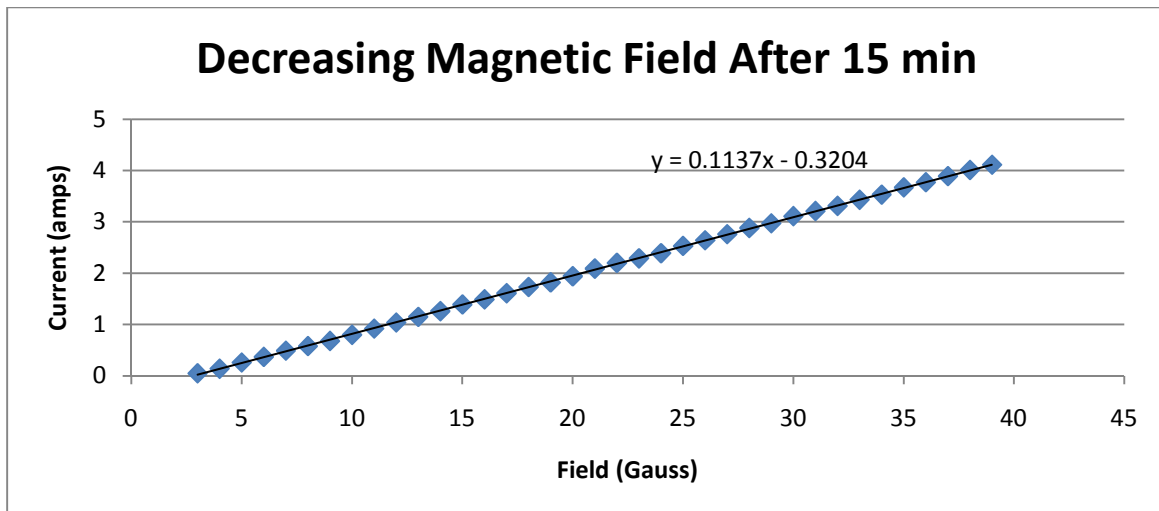
Figure 5: Magnetic field calibration[2].

[2] This magnetic field calibration is used for all experiments listed. It was also periodically verified to ensure reproducibility for all experimental data. The Helmholtz Coil has an intrinsic magnetic field without any current flow due to hysteresis.

V. Amplitude and Signal-Shape Test Using an Oscilloscope

The first magnetic field tests were performed with a focus on the amplitude of the anode signal under varying field strengths. The desire was to find the point where the magnetic field had a strong impact on the degradation of the ADC signal.

A 5-mm thick piece of scintillation material is attached to the photocathode end of the PMT using a combination of tape and optical gel. The PMT and scintillator are both wrapped in two layers of Tedlar film, which provides a light tight environment to ensure that the only photons reaching the photocathode come from the scintillator.

A Strontium-90 source is placed on the scintillator end of the PMT. The Sr-90 β^- decay releases electrons. These electrons excite the scintillation material, which releases photons while returning to its ground state. The photons interact with the photocathode of the PMT through the photoelectric effect, resulting in the emission of electrons. The anode signal from the PMT, once the electrons have passed through the electron-multiplier section as outlined previously[3], is proportional to the number of photons emitted from the scintillator.

The PMT is then placed inside a Helmholtz Coil, which provides varying magnetic field strengths. A wooden table attached to a metal stand keeps the PMT in the center of the coils, and also allows for the PMT to be rotated to achieve different magnetic field

---

[3] See The Electron-Multiplier Section on pg. 5.

geometries. The PMT is held in place with rubber bands to keep it from rolling off the

table. The strength of the magnetic field is adjusted using a current source properly

calibrated to the desired magnetic fields measured with a Gauss Meter[4]. The high

voltage input to the PMT is held consistent for the entire experiment using a Glasman

High-Voltage Generator.

The PMTs used in this experiment are Hamamatsu R9779 models with and

without magnetic shielding, starting with the ladder. Before a magnetic field is applied,

the scope shows an average amplitude of around one volt, found by averaging signals

over 128 samples per second, when the trigger is set to -200mV. The magnetic field is

then set to 30 G and "warms up" for fifteen minutes at the start of the test. The

amplitude readout on the scope is saved as a jpeg image for comparison after the test.

Once the data has been saved, the magnetic field is reduced by 2 G and data is taken

again. This procedure is repeated until the magnetic field is 2 G. This is the intrinsic

magnetic field in the Helmholtz Coil due to the hysteresis of the material of the actual

setup. Figure 6 shows an example of the jpeg images saved during the experiment.

---

[4] See Magnetic Field Calibration on pg. 7.
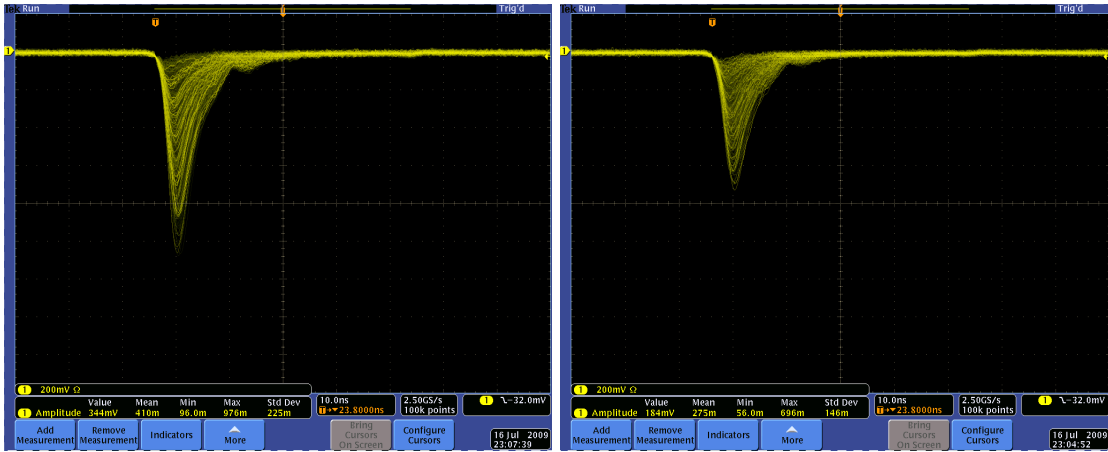
Figure 6: Analog signal of the R9779 PMT without shielding with no magnetic field (left) and with a 12 G axial field (right)[5].

The results show consistent analog signal reduction as the axial magnetic field increases. This method for testing was abandoned, however, because the sampling depth of the scope for averaging the amplitude of the analog signal is not high enough to yield reproducible results. The test did reveal, however, that the signal shape is preserved under varying magnetic fields, which already indicates that the time resolution measurements will not be impacted by any detrimental pulse deformations. Because the pulse shape is preserved, the signal amplitude alone serves as a measure of the field's impact. A reproducible method for measuring the amplitude is needed.

---

[5] The amplitude of the signal has been reduced, but the shape remains unchanged.

VI.   Signal-Reduction Measurements

The experiment is designed to investigate the effects of varying magnetic-field strengths and geometries on the photomultiplier tubes that will be used for the TOF12 detector at Jefferson National Lab. The same PMT detector, Sr-90 source, and Helmholtz Coil from the amplitude test described before are used again. To achieve reproducible results, a three step process takes the analog signal from the PMT and outputs a histogram showing the distribution of the total charge. The PMT provides the initial analog current signal. This is then read by the CAMAC[6] (Lecroy 1434A) and NIM[7] (Phillips Scientific 700) electronic system. A computer program then reads the data and outputs a histogram using ROOT[8].

CAMAC Module Descriptions

a. ADC (LeCroy 2249W)

The Analog to Digital Converter (ADC) calculates the area of the analog signal, which is directly proportional to the number of photons emitted from the scintillator. The unit features a gate, or a specific time interval over which the ADC integrates the incoming analog current signal to find the total charge. The gate width is adjusted using a logical signal, which "opens" the gate when true and keeps the gate "closed" when false. There are twelve input channels on the ADC, and each can be adjusted with an

---

[6] Computer Automated Measurement and Control.
[7] Nuclear Instrumentation Module.
[8] A C++ based environment used for data analysis.

offset (an additional charge added to the integrated signal). The ADC stores the integrated charge value in a file on the computer.

b. Output Register (CAEN C219)

The output register relays a signal once the data collection process between the computer and ADC is complete. This will allow another signal from the PMT to reach the electronics for further analysis.

NIM Module Descriptions

a. Leading-Edge Discriminator (Phillips 705)

The discriminator converts an analog signal into a NIM logical signal. There are two main adjustments that can be made to each channel on the discriminator. The threshold (variable from -10mV to -1V) determines when the analog signal triggers the output logical signal. The width of the logic signal can also be adjusted. In this experiment, the width of this logic signal directly determines the size of the gate at the ADC. A veto input on the discriminator prevents any additional logical signals from leaving the discriminator until it has been reset.

b. Logic Fan-In/Fan-Out (EG&G-ESN LF4000)

The logic Fan-In/Fan-Out allows a single logical signal to be split into several outputs.

c. Quad Gate/Delay Unit (Phillips 794)

The Quad Gate/Delay Unit serves multiple purposes. It generates a timed pulse that is used to open an accidental gate at the ADC to analyze the offset positions. The

unit also features a Flip-Flop function, which is used in the experiment for the veto input of the discriminator to prevent additional events from being processed.

d. Scaler (SIN S-101)

The scaler simply shows the number of events recorded by the digital readout. It receives its input from the logic Fan-In/Fan-Out.
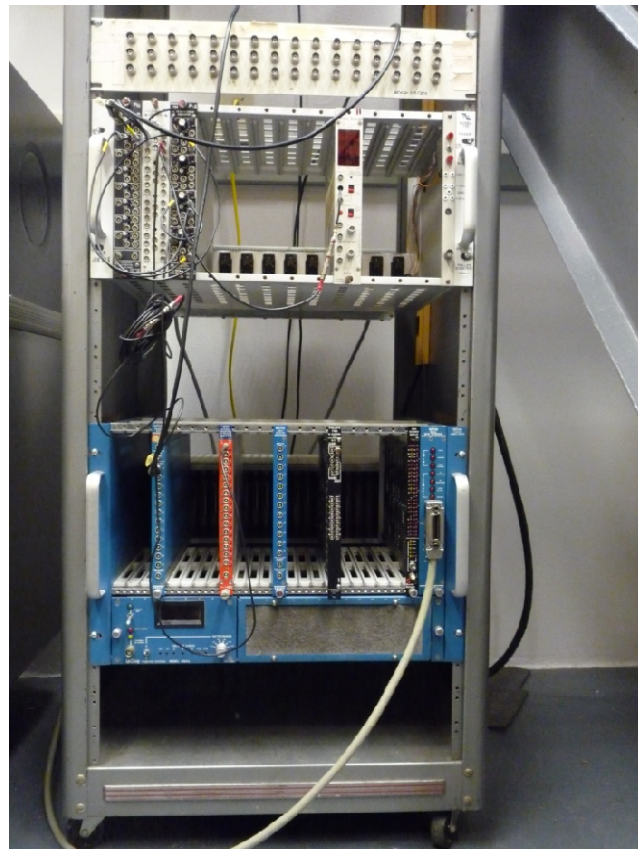

Figure 7: CAMAC (top) and NIM (bottom).

Electronics Description

Figure 8 shows the schematic for the electronics of the experiment. The PMT features an anode and dynode signal output. The anode signal is fed directly into the ADC input of the CAMAC for analysis. The dynode feeds into a leading-edge discriminator, where the analog signal is converted into a logical signal. The logical signal from the discriminator is fed into a logic Fan-In/Fan-Out, which splits it into several identical signals. One of these split signals sets an event Flip-Flop, which sends a veto signal to the discriminator. This prevents the discriminator from generating any further signals until the Flip-Flop is reset. The reset signal is generated by the CAMAC output register as soon as the computer has finished the read out and sends a computer-ready signal. Another signal from the Fan-In/Fan-Out generates the ADC gate. The gate defines the time window in which the ADC integrates the analog signal from the PMT. The final output from the Fan-In/Fan-Out runs into a scaler to count the number of events during the experiment. The ADC value is read by the computer via the CAMAC controller. When the processing of the data is complete, the output register sends a computer-ready signal, resetting the Flip-Flop and allowing another logical signal to leave the discriminator.
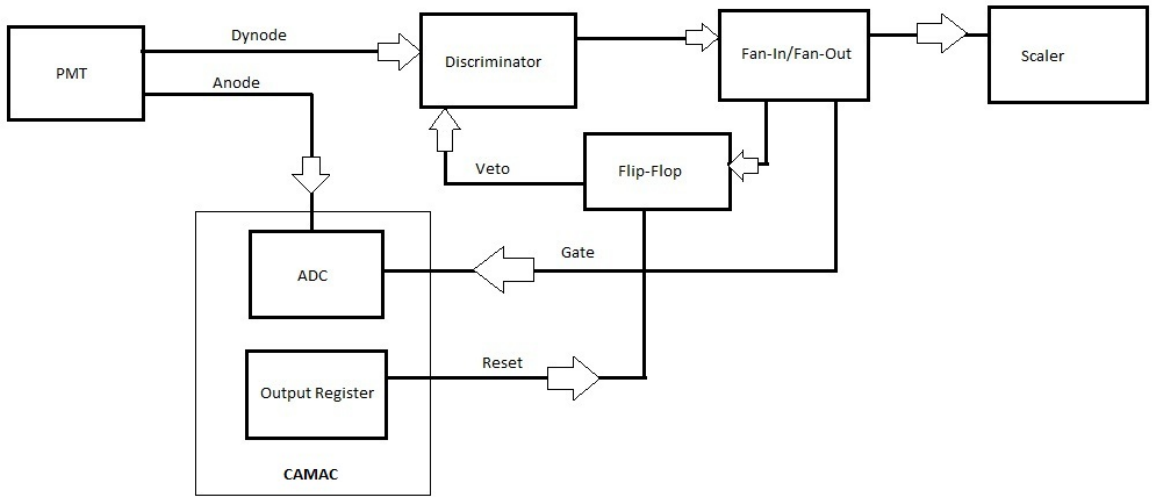
C++ Program for Data Acquisition

The first channel is used on the ADC for data acquisition. A C++ program is needed to properly read the data file and populate a histogram in ROOT. This program places the data in an array and then into a histogram. The program reads in the ADC values, which are formatted into a text file filled with data by the computer, and allows for easy access to data files created by the computer. Only the first thirty-thousand and one events are read in by the program to ensure that the statistics for each experiment are consistent with each other. This program will continue to be used for additional research opportunities for students working in the NGB.
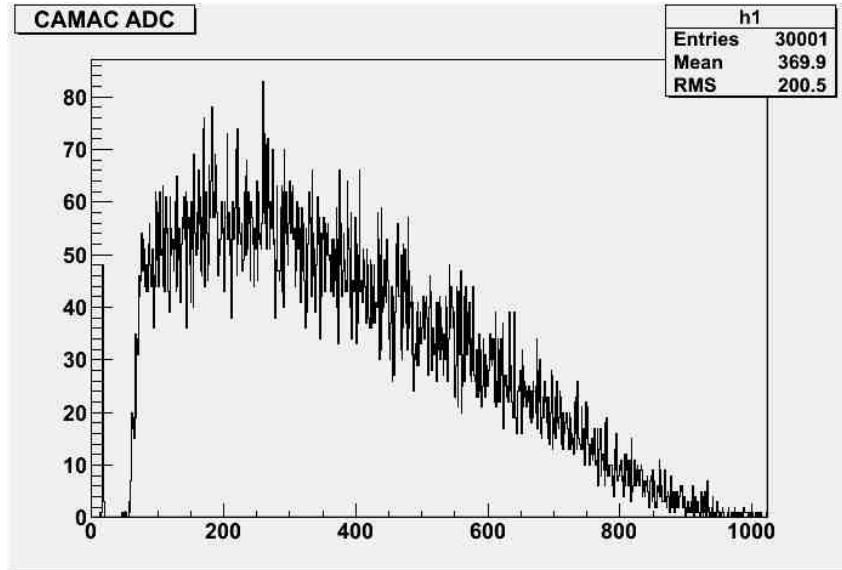
Electronic Calibration

Before conducting the magnetic-field testing, the electronics used for the data acquisition must be properly calibrated. The high-voltage controls the PMT output signal, giving the ADC value and thus populating the histogram. The high voltage must be adjusted to populate the full dynamic ADC range. The ADC offset must be calibrated so that it is visible but no reducing the dynamic range of the ADC. Finally, the threshold of the discriminator must be lowered to read the lowest analog signals without being impacted by the noise of the electronics, while the width of the generated logical signal is set to integrate the entire analog signal.

a. High-Voltage Adjustment

The high-voltage input into the PMT must be adjusted so that the ADC signal covers the full range of the histogram. Care must be taken, however, so that the high voltage does not exceed the limit specified for the PMT. Each PMT used in the

17

experiment must be individually calibrated to a proper high-voltage input. This is

similarly done in the three-bar-method[9] to ensure that the ADC readout on each PMT is

consistent with the full dynamic range of the ADC signals over the length of the

scintillation bar. The proper high voltage varies from PMT to PMT, but is commonly

around 1.5 kV.
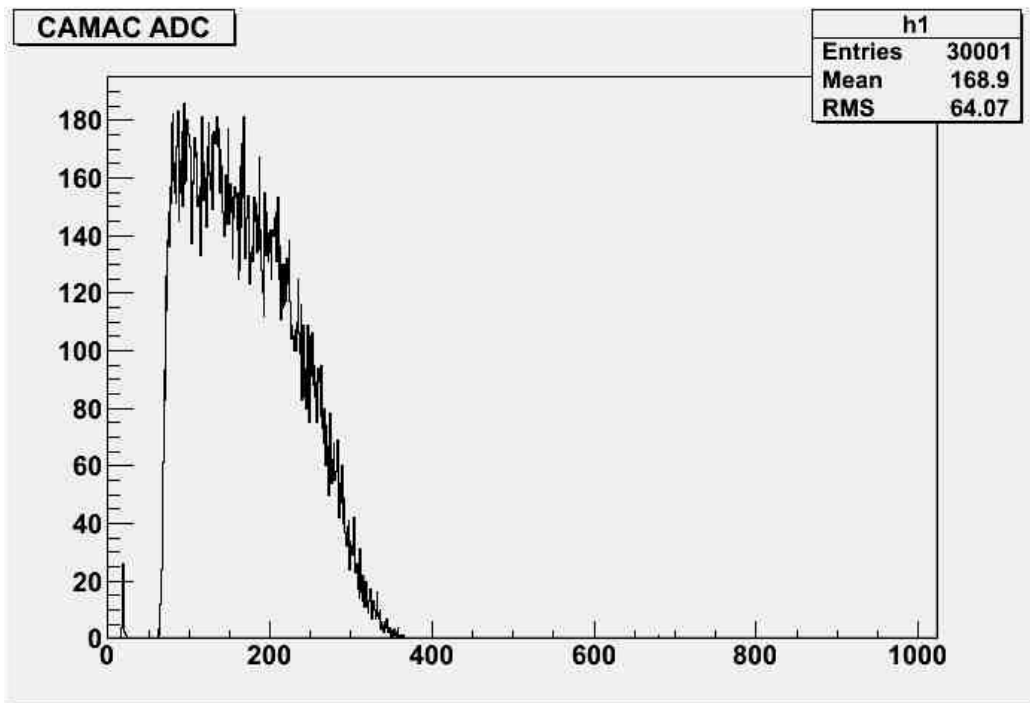
Figure 10: ADC signal before high-voltage calibration[10].

b. ADC-Offset Calibration and Pedestal

The ADC has an additional amount of charge which it adds to the integrated

signal under the gate generated by the internal electronics of the ADC. This is called the

pedestal, and can be adjusted on the actual ADC module to desired values. The offset

also includes signal offsets and noise generated by external sources. It should be

---

[9] See Time Resolution pg. 38.
[10] The X-axis represents the integrated analog signal, and the Y-axis records the number of events.

lowered as much as reasonably possible in order to preserve the full dynamic range of all signals. The random gate generated by the NIM electronics is used to measure the offset during the experiment by integrating the analog signal during time windows that are not correlated to detected β^- events. To actually extract the integrated analog signal, this offset must be known and subtracted from the ADC value.
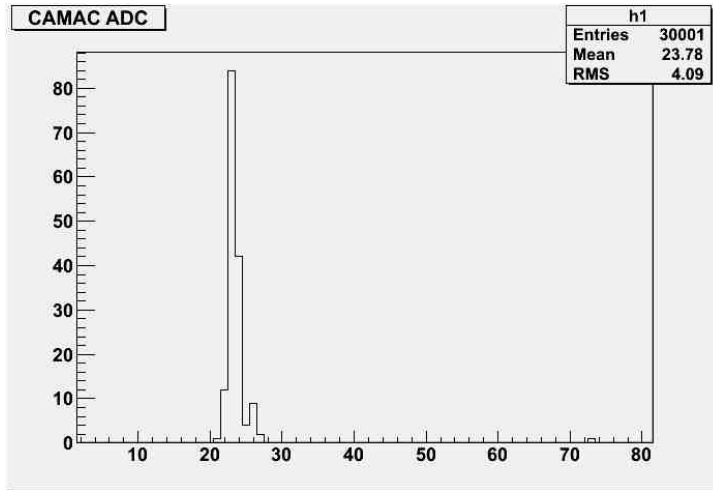
c. Discriminator Threshold and Width

The leading-edge discriminator features two adjustable features: the threshold and width. The threshold indicates the smallest signal amplitude that triggers the discriminator to send out a logical signal. The goal is to lower the threshold to register the low energy deposits and hence small ADC values while ensuring the discriminator is not triggered by the noise. The gate width on the discriminator must also be adjusted because it is used to open the gate on the ADC for signal integration after it has passed through the Fan-In/Fan-Out.
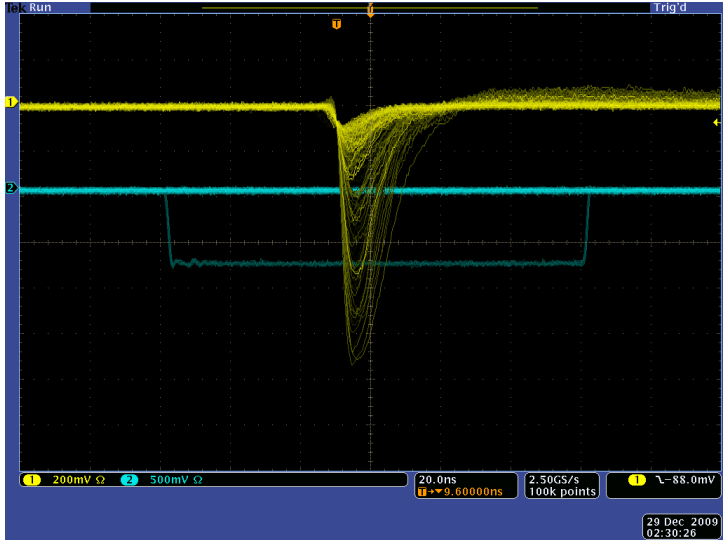
Figure 12: Logical gate (bottom) and analog signal (top)[11].

The gate width on the ADC must be large enough to fit the entire analog signal from the PMT, as seen in Figure 12. This is done by adjusting the gate width on the discriminator. There must also be compensation for the time delay introduced by the NIM electronics, which will have an effect on when the gate is opened on the ADC. In addition, the wire delay of the analog signal has to be adjusted to that the gate is opened at least 30ns before the PMT analog signal arrives to ensure that the ADC is ready for integration.

---

[11] Any portion of the analog signal outside the logic date will not contribute to the ADC measurement. The solid line above the logic gate is due to the fact the oscilloscope is triggering on the analog signal.

Magnetic-Field Test on PMT without Shielding

The PMT is placed inside of the Helmholtz Coil in the same manner as the earlier oscilloscope test[12]. The previously mentioned electronics outline[13] for the NIM and CAMAC system allows for the data analysis of the analog signal. The magnetic field is initially set to 10 G for an axial alignment with the photomultiplier tube. After "cooking" the magnetic field for fifteen minutes, the CAMAC read out is turned on for data acquisition. Each experiment takes around a half-hour to complete. Figure 13 shows a comparison between ADC distributions. The histogram for the 10 G axial magnetic field test shows a reduction in the ADC signal of around 10%[14]. This signal reduction does confirm anticipated effects of magnetic fields on PMTs as well as the quantitative findings from the earlier oscilloscope test.
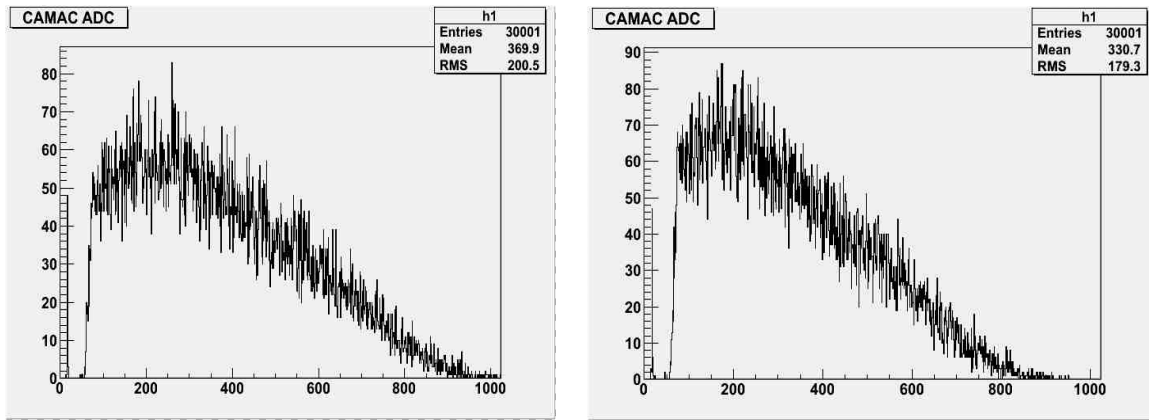
Figure 13: No magnetic field (left) and 10 G axial field (right).

---

[12]See Amplitude and Signal-Shape Test Using an Oscilloscope on pg. 9.
[13] See Figure 8 on pg. 16.
[14] This can be done by comparing the mean values on the histogram.

The PMT is then turned by 90° to analyze the effects of transverse fields on the PMT.

The ADC signal is completely lost under a 10 G transverse field. These results indicate

that transverse magnetic fields must be properly shielded in order to preserve a

measurable ADC signal.

VII.   Mu-Metal Shielding

Materials with high-magnetic permeability shield the effects of magnetic fields.

Mu metal features a very high magnetic permeability, around 80,000 – 100,000

compared to only several thousand for steel. A layer of mu metal is commonly wrapped

around a PMT in order to prevent PMT signal loss in the presence of magnetic fields.

The magnetic field tests conducted in the Helmholtz Coil were repeated using a PMT

with mu-metal shielding already built in.

Figure 14: PMT with mu-metal shielding (left) and without shielding (right)[15].

---

[15] The black region on the left PMT is mu-metal shielded. The shielding no longer allows for verification of the dynode arrangement inside. The PMTs are both Hamamatsu R9779s, but the one on the left has been modified with mu-metal shielding.

Magnetic-Field Test of a PMT with Mu-Metal Shielding Built In

The mu-metal shielded PMT is placed in the Helmholtz Coil in the same manner as the previous tests and using the exact same electronics setup in the CAMAC and NIM crates[16]. The magnetic field is once again set to 10 G, and data is taken for axial and transverse magnetic fields. The axial field results are similar to those using non-shielded PMTs: there is a loss of around 10% in the PMT signal. This was already anticipated because the mu-metal shielding is only present on the casing of the PMT and not the photocathode to which is attached to the scintillation material. The mu-metal shielding cannot extend over the photocathode to achieve the design requirements for the acceptance. The complete ADC distribution is, on the other hand, still preserved when a transverse field is applied. This already shows the mu-metal shielding built into the PMT is adequate for transverse fields of 10 G.

---

[16] See Figure 8 on pg. 16.
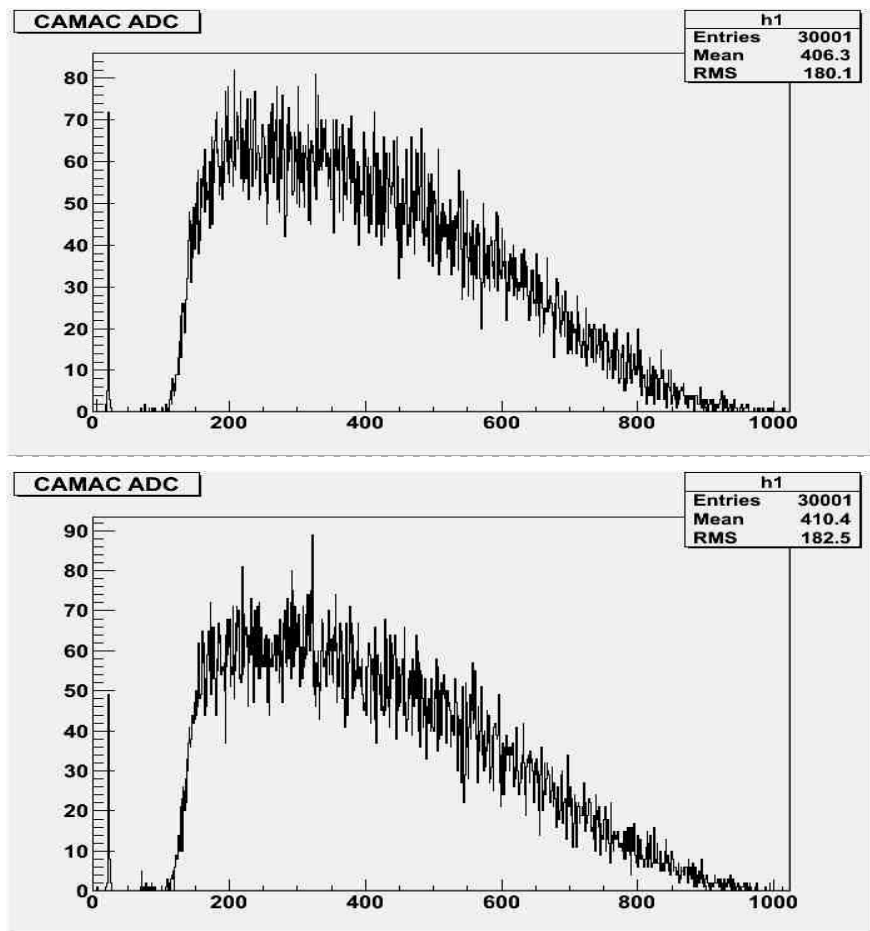
Figure 15: PMT with mu-metal shielding with no magnetic field (top) and a 10 G transverse field (bottom).

The magnetic-field is then increased in order to observe the effectiveness of the shielding. The PMT signal continues to deteriorate as the axial-field strength increases. The transverse magnetic field only begins to have an effect on the PMT signal when it reaches around 20 G. The mu-metal shielding in the PMT is enough to shield the PMT signal until transverse-magnetic fields reach 20 G. Once the transverse magnetic field exceeds 20 G there is a rapid deterioration of the PMT signal.
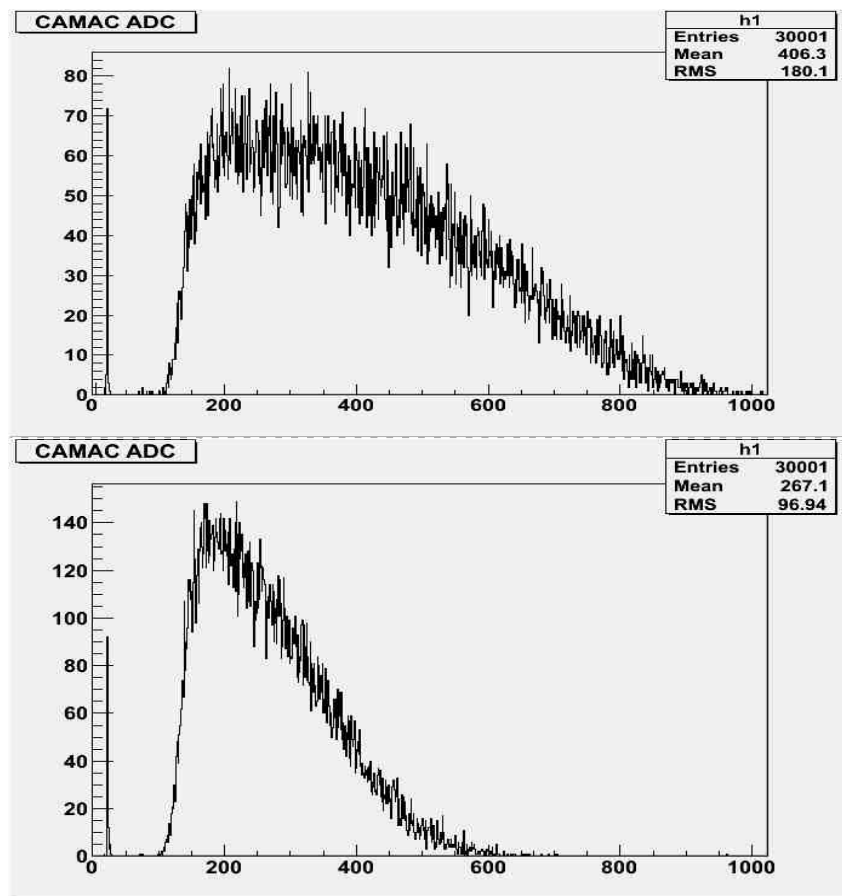
**Figure 16: No magnetic field (top) and a 20 G axial field (bottom).**
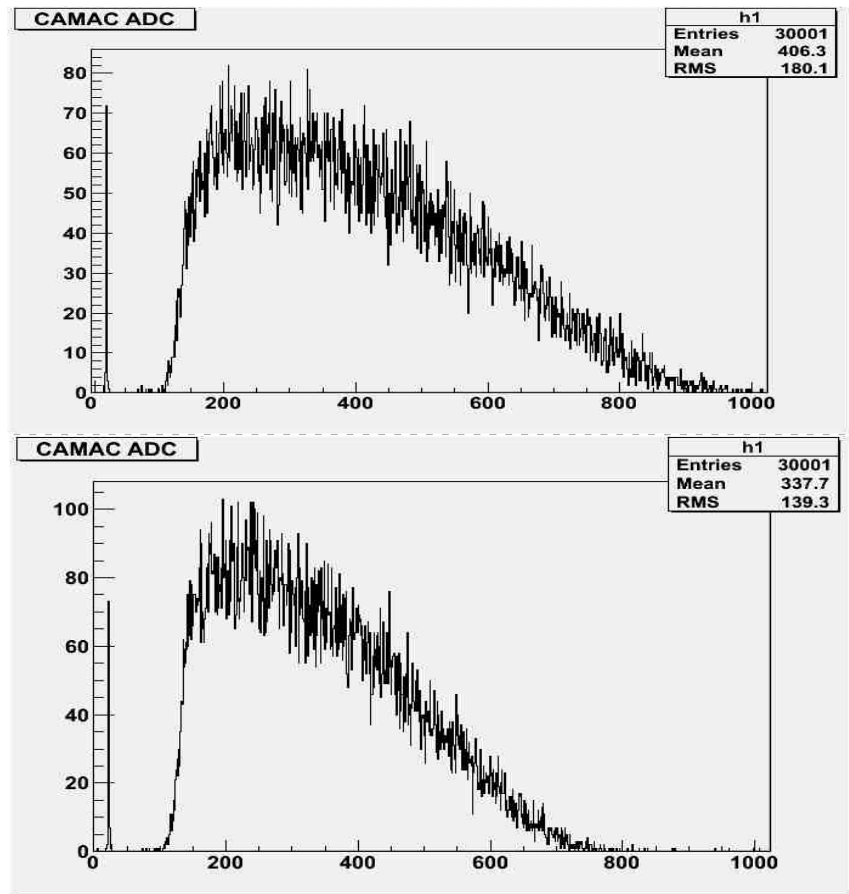
**Figure 17: No magnetic field (top) and a 20 G transverse field (bottom).**
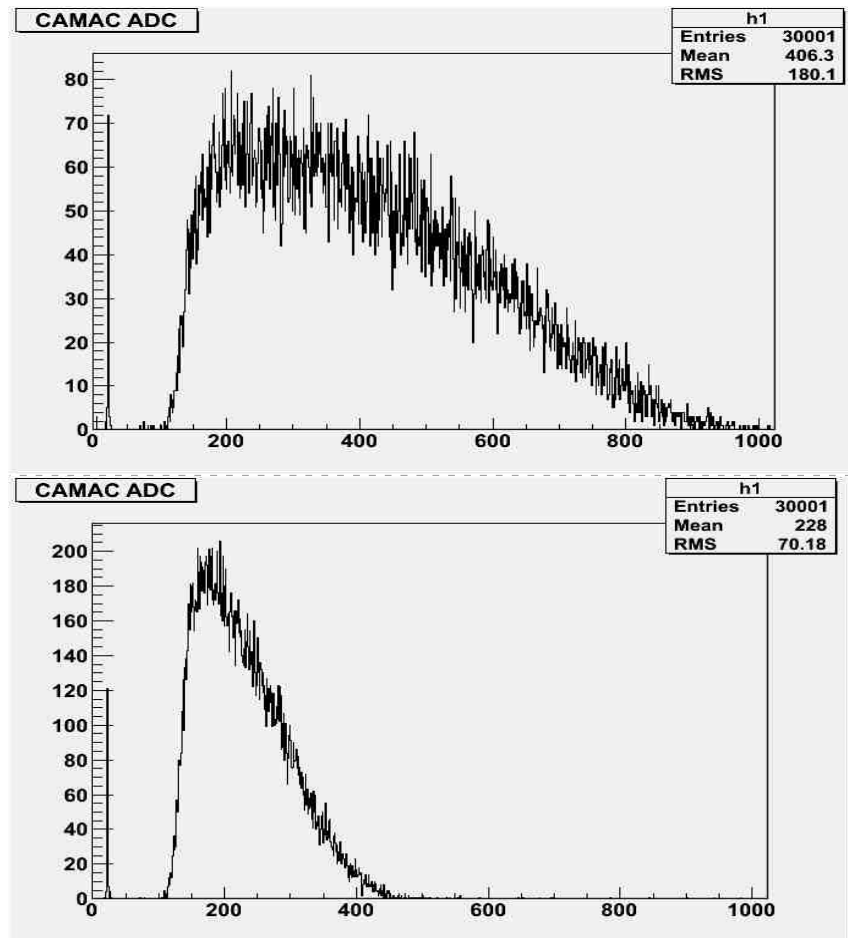
Figure 18: No magnetic field (top) and a 25 G transverse field (bottom).

VIII. Further Shielding Methods

The strength of the magnetic field at Jefferson Lab has yet to be determined, though it will supposedly be below 20 G. While awaiting the final values, the University of South Carolina has been exploring alternative methods for shielding the PMTs from higher than expected magnetic fields. Two options can further shield the PMTs from magnetic fields.

Additional Mu-Metal Shielding

The construction designs for the FTOF detector at Jefferson National Lab allows for additional mu-metal shielding for the PMTs if the magnetic field intensity proves larger than expected. Many different configurations of shielding can be used, though the current design decision is based on a rectangular box which will cover the PMT to the actual scintillator. It is important not to cover the scintillator with mu metal because the counters are stacked and would require trimming to fit the additional shielding. The width of the box used in the experiment can be adjusted by adding additional mu-metal plating along the four sides and the end piece encapsulating the PMT as needed by the design. Figure 19 shows the shielding design schematic and, for the purposes of this experiment, the sides are 2 mm thick, while the end piece is 5 mm.
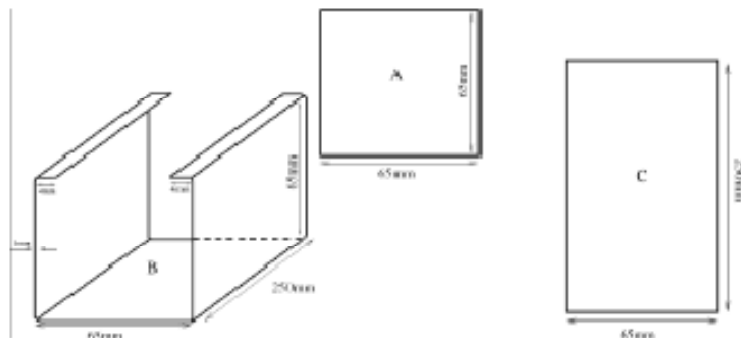
Figure 19: Mu-metal shielding schematic used during testing.

The magnetic field is adjusted to 25 G to once again analyze the effects of large transverse fields. The ADC distribution shows that the signal has been preserved even under transverse fields with the additional mu-metal shielding surrounding the PMT. The axial fields, however, are not shielded by this mu-metal shield. This, again, makes sense, because the axial fields are incident on the photocathode, where there is no shielding. It was hoped that the thick end plate on the mu-metal box would help to shield against the axial fields, but this was not the case.
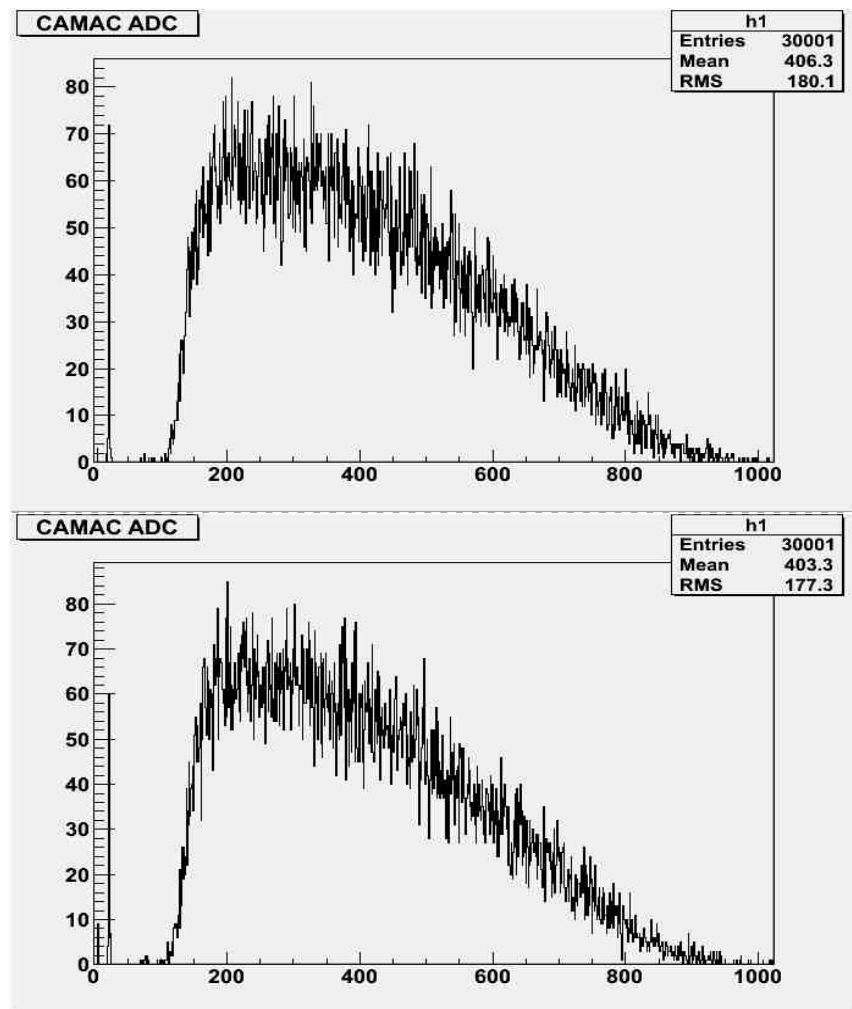
**Figure 20: No magnetic field (top) and additional shielding and a 25 G transverse field (bottom).**

Active Shielding

There are further options for shielding the PMTs from axial fields. One option is to apply active shielding to the PMT by wrapping it in a coil and running a current through. This will create a magnetic field which should counteract the axial fields inside the FTOF detector. Without knowing the exact magnetic field values, however, no final decisions can be made at this time. The group in charge of the magnetic field calculations at Jefferson Lab must supply the University of South Carolina with the final estimate values in order to finalize the construction process of the PMTs as well as the need for additional shielding on site.

IX. Analyzing the Cylindrical Symmetry of the PMT

Because the scintillators at Jefferson Lab will be placed in varying positions around the torus magnet in the detector, verification of symmetry effects in the magnetic fields are necessary.

Symmetry along the R-Axis

Consider the PMT to be a standard cylinder with the z-axis giving the axial symmetry. Rotations around the resultant perpendicular axis (r-axis) should to first order yield symmetric results.

A PMT with mu-metal shielding built in is placed on a turntable, which also measures the angle of rotation about the r-axis perpendicular to the z-axis running through the PMT. A magnetic field strength of 20 G and no additional shielding is used because this should show a great deal of impact on the ADC distribution. The magnetic field begins with axial impact on the photocathode, which is calibrated to zero degrees. Once data has been taken, the turntable is rotated ten degrees and another measurement is carried out. This process repeated until the turntable is rotated a full 180 degrees. The turntable angle measurement has 2-3 degrees error. The data collected show that the r-axis rotation does indeed show some symmetry when the error of the magnetic field strength and of the turntable angle is taken into account.
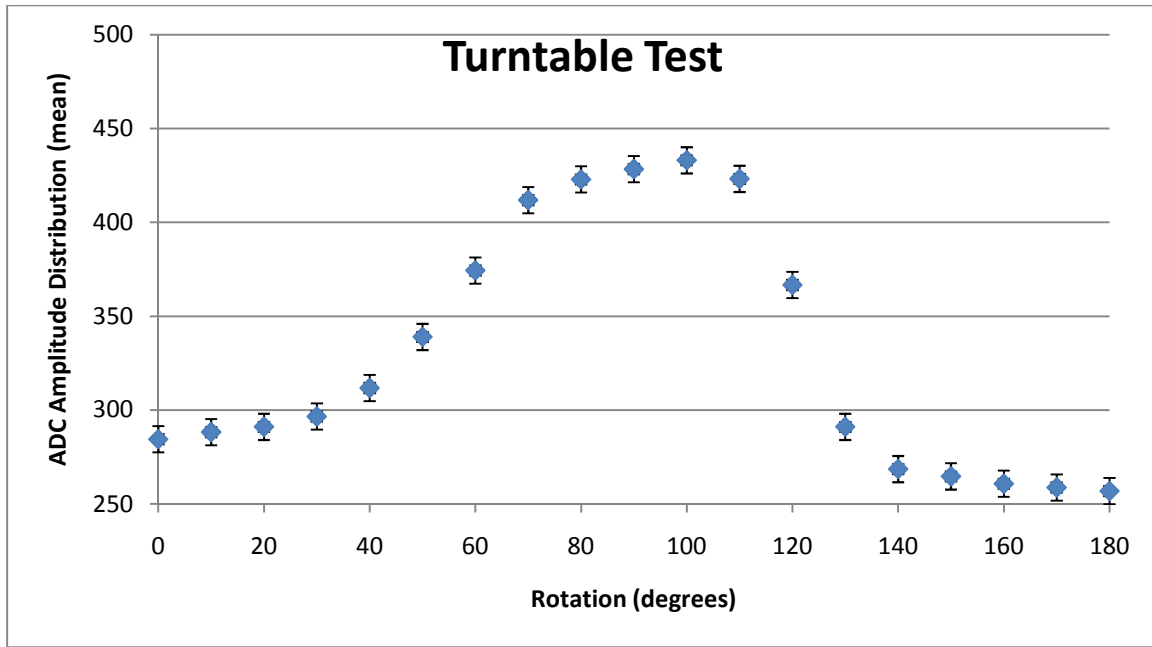
Figure 21: R-axis rotations[17].

Symmetry along the Z-Axis

While the turntable test verified the first order symmetry of the mean along the perpendicular axis of rotation of the PMT the data collected under the transverse magnetic field did not match previous results under the same 20 G magnetic field. The ADC signal do not show a consistent signal reduction as was expected.

For better analysis, the PMT is placed inside the Helmholtz Coil to create a transverse field similar to the r-axis test. The anode signal is read out on an oscilloscope for real time analysis. A mark is made on the PMT to measure the azimuthal angle. The PMT is then rotated to investigate changes in the signal. The PMT dynode arrangement does not appear to have axial symmetry. There is a maximum position which shows a completely shielded anode signal, as well as a minimum that shows the most signal degradation, as illustrated in Figure 22. This can best be explained by the dynode

---

[17] The Y-axis shows the mean of the ADC distribution.

arrangement inside the PMT. Without knowing the exact dynode arrangement, the

PMTs must each be individually tested during construction of the detectors to ensure

the maximum and minimum positions are determined and marked. The magnetic field

is then reduced to see when the ADC signal is restored at the minimum position, and it

is found to be around 14 G. It is important to note that even with this drop in PMT

signal at the minimum position, the mu metal in the PMT is still providing ample

shielding, when compared to a complete signal loss in the PMT without shielding under

10 G transverse fields. To ensure that this phenomenon was not a result of a poorly

constructed PMT, other PMTs were tested in the exact same setup and yielded

consistent results.

While still in its minimum orientation, the PMT is placed inside of a mu-metal

box. The PMT signal is now fully restored, once again showing the importance of the

mu-metal shielding for the CLAS-12 detector.
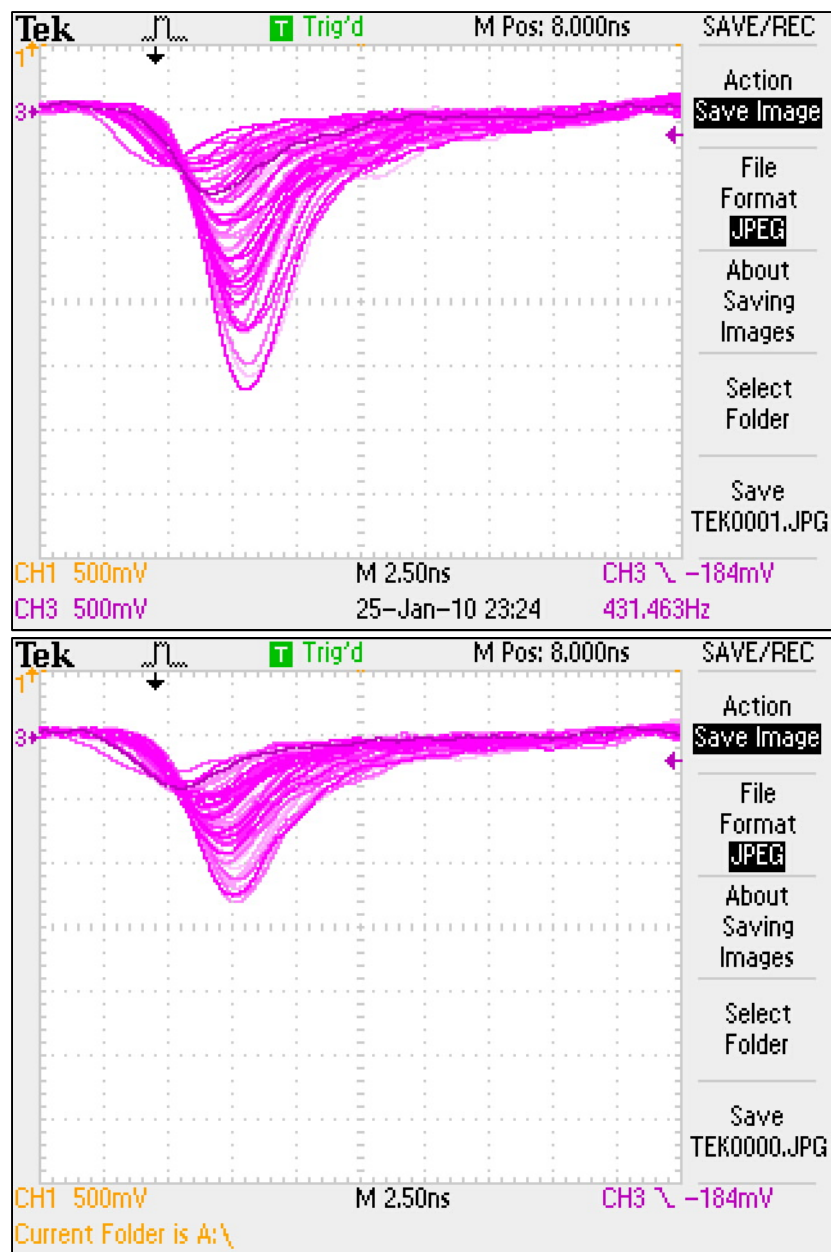
Figure 22: Maximum ADC position (top) and minimum ADC position (bottom) under a 20 G transverse field.

X.   Time Resolution

Particle identification in the CLAS 12 Detector is accomplished through the Time of Flight (TOF) system. TOF measures the time it takes for a particle to travel from its starting position to where it is detected inside CLAS. This allows for the calculation of the particle's speed, and together with the knowledge of its momentum this leads to particle identification. The TOF system must be extremely accurate, meaning the time resolution, or the smallest time interval that can be measured accurately (Leo, 1987), must be very small. The CLAS-6 detector currently features time resolution of around 120ps. The CLAS-12 detector on the other hand must achieve a time resolution below 80ps to accurately identify particles.

Counter Construction

The University of South Carolina has been tasked with constructing the TOF counters for CLAS-12. Each counter consists of a long plastic scintillator with PMTs attached to both ends. The scintillator is wrapped in an aluminized mylar film to reflect photons from the scintillator back inside to reach the PMTs. After wrapping the scintillator in Tedlar film to provide a light-tight environment, the PMTs are attached to the ends with optical grease in a similar fashion to the previous magnetic field

experimental setup[18]. For the time resolution tests presented here, the scintillators are

6cmX6cmX120cm Bicron BC-404 and the PMTs are Hamamatsu R9779.

Three-Bar Cosmic-Ray Method

Each counter constructed at USC for TOF must be tested to ensure the desired

time resolution. Three scintillation detectors are spaced evenly and aligned vertically.

The top and bottom counters are of known time resolution. The middle bar is

exchangeable, and each counter for TOF will be placed in this position to measure the

time resolution. Cosmic rays travel through the three scintillators, triggering all six

PMTs in the experiment.
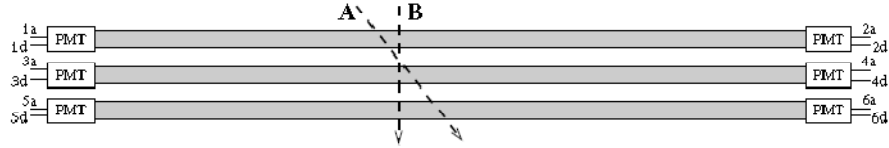
Figure 23: Three-bar-method with identical counters.

The equal spacing of the bars ensures $T = \frac{t_t + t_b}{2} - t_m = constant$, where

the subscript denotes top, bottom, and middle. The individual times for counters can be

written in terms of their left and right PMT times as follows:

$$t_l = \frac{t_{tl} - t_{tr}}{2} = \frac{t_1 + t_2 - 2t_{ref}}{2},$$

$$t_m = \frac{t_{ml} - t_{mr}}{2} = \frac{t_3 + t_4 - 2t_{ref}}{2},$$

$$t_b = \frac{t_{bl} - t_{br}}{2} = \frac{t_5 + t_6 - 2t_{ref}}{2},$$

where the reference time will finally cancel out when simplified to

---

[18] See Amplitude and Signal-Shape Test Using an Oscilloscope on pg. 9.

$$T = \frac{t_1 + t_2 + t_5 + t_6 - 4t_{ref}}{4} - \frac{t_3 + t_4 - 2t_{ref}}{2}$$

$$= \frac{t_1 + t_2 + t_5 + t_6}{4} - \frac{t_3 + t_4}{2}.$$

The spreading of T is quantified by the standard deviation σ_T, and can also be compared

to the standard deviation for each individual PMT i.

$$\sigma_T^2 = \frac{1}{16}(\sigma_1^2 + \sigma_2^2 + \sigma_5^2 + \sigma_6^2) + \frac{1}{4}(\sigma_3^2 + \sigma_4^2)$$

Each counter is constructed with the same PMTs, implying the impact on the time

resolution is the same

$$\sigma_{1,2} = \sigma_1 = \sigma_2$$

$$\sigma_{3,4} = \sigma_3 = \sigma_4$$

$$\sigma_{5,6} = \sigma_5 = \sigma_6$$

In addition, the reference counters for top and bottom are the same,

$$\sigma_{1,2} = \sigma_{5,6},$$

and the resolution of each counter is given by

$$\sigma_{counter} = \frac{1}{\sqrt{2}}\sigma_{PMT}.$$

The measured value of the middle counter can now be found using the measured σ_T

and

$$\sigma_T^2 = \frac{1}{16}4\sigma_{1,2}^2 + \frac{1}{4}2\sigma_{3,4}^2$$

with $\sigma_r = \sigma_t = \sigma_b$ follows that

$$\sigma_T^2 = \frac{1}{16}4(\sqrt{2}\sigma_r)^2 + \frac{1}{4}2(\sqrt{2}\sigma_m)^2$$

and

$$\sigma_T^2 = \frac{1}{2}\sigma_r^2 + \sigma_m^2$$

finally leading to

$$\sigma_m = \sqrt{\sigma_T^2 - \frac{1}{2}\sigma_r^2}.$$

This allows us to easily calculate the time resolution for each bar swapped in the middle of our arrangement. When all three bars are the same $(\sigma_r = \sigma_t = \sigma_b = \sigma_m)$, then the time resolution is given by $\sigma = \sqrt{\frac{2}{3}}\sigma_T$ (Gothe, Phelps, Steinman, & Tian, 2009).

Electronics Description

The electronics for the time-resolution measurements is comparable to the magnetic field tests. An added time to digital converter (TDC) module measures the time of the arriving signal from each PMT.
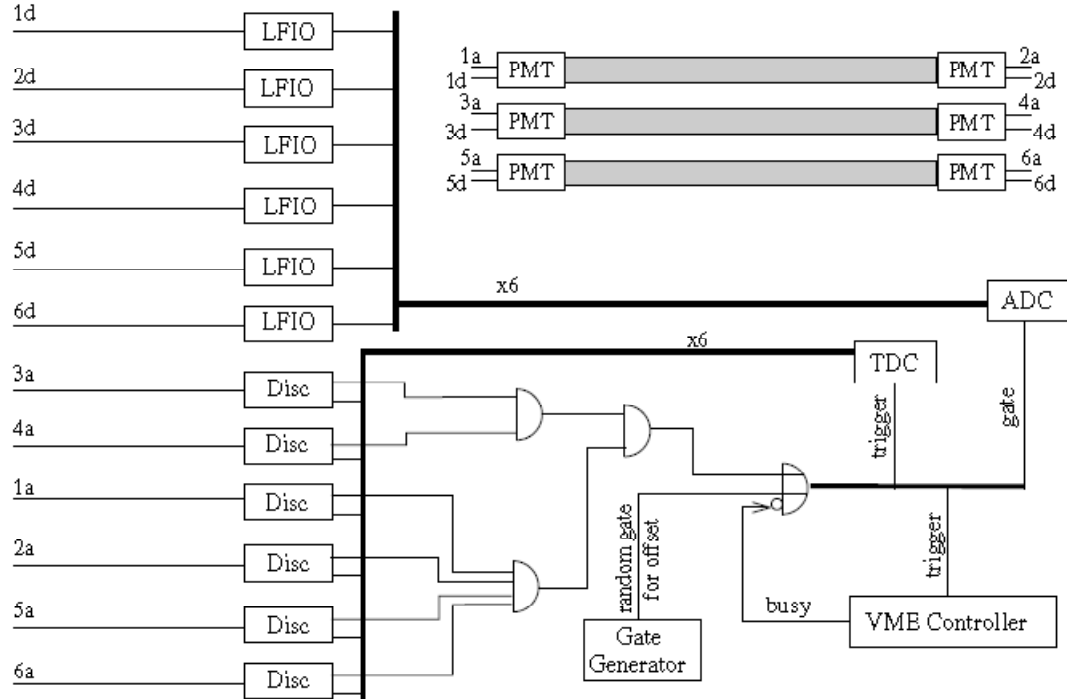
Figure 24: Electronic schematic for time resolution.

The dynode signals from the PMTs lead into the Linear Fan-In/Fan-Out (LFIO),

while the anode signals go to the Lecroy 623B Leading-Edge Discriminator. A Phillips

Scientific 755 Quad Logic and Lecroy 622 Coincidence units work in tandem to detect

when a particle has passed through all three bars. Channel three and four refer to the

left and right sides of the middle bar respectively, and their logical signals from the

discriminator run into a two-fold coincidence unit. The four-fold coincidences from the

remaining PMTs in the top and bottom bars are then led into a six-fold coincidence,

which indicates a cosmic ray passed through all three counters, and opens the gate on

the ADC and sets the TDC trigger. The ADC and TDC data for such an event are then

read out and stored in a file for data analysis.

Time Resolution Cuts

Two cuts are used in the time-resolution measurement. The goal is to accurately

measure the time resolution while maintaining as many events as possible.

a. TDC-Center Cuts

The difference in the TDC values gives the position of the particle in the

scintillator. Initially, the time resolution measurements are done with particles passing

through the center of each bar by cutting on the center of the TDC difference histogram.

Cutting along TDC difference values allows the time resolution for various positions

inside the scintillator to be determined.
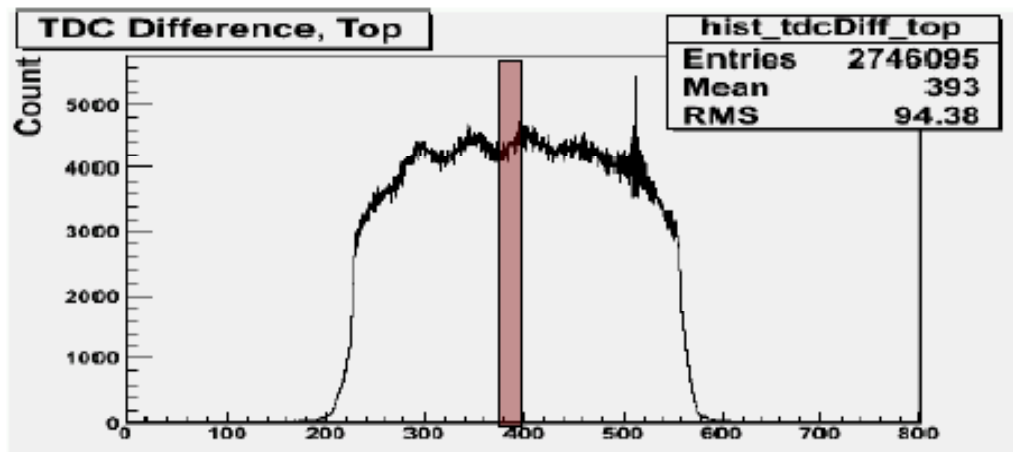
Figure 25: The TDC-center cut (shaded)[19].

---

[19] The shaded region used in the time resolution measurement can be moved to different positions along the counter.

b. ADC Cuts

The TDC-center cuts do not prevent particles from passing through small regions on one or more bars because of their incoming trajectory, as seen in Figure 26. The corresponding ADC values would be comparatively small, and thus detrimentally effect the time resolution measurement.
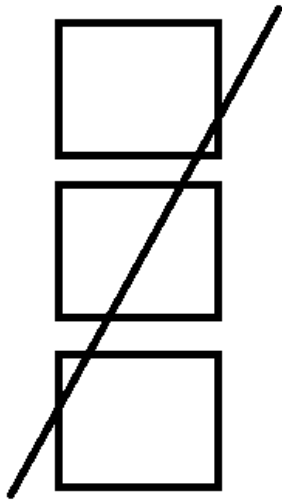

Figure 26: Possible particle trajectory.

For the three-bar-method time-resolution measurements the lowest ADC values must be cut away to prevent them from smearing the actual time resolution that will be seen at Jefferson Lab. These ADC cuts will not be necessary for the final FTOF detector, because the spherical design and stacked geometry will prevent such an occurrence.
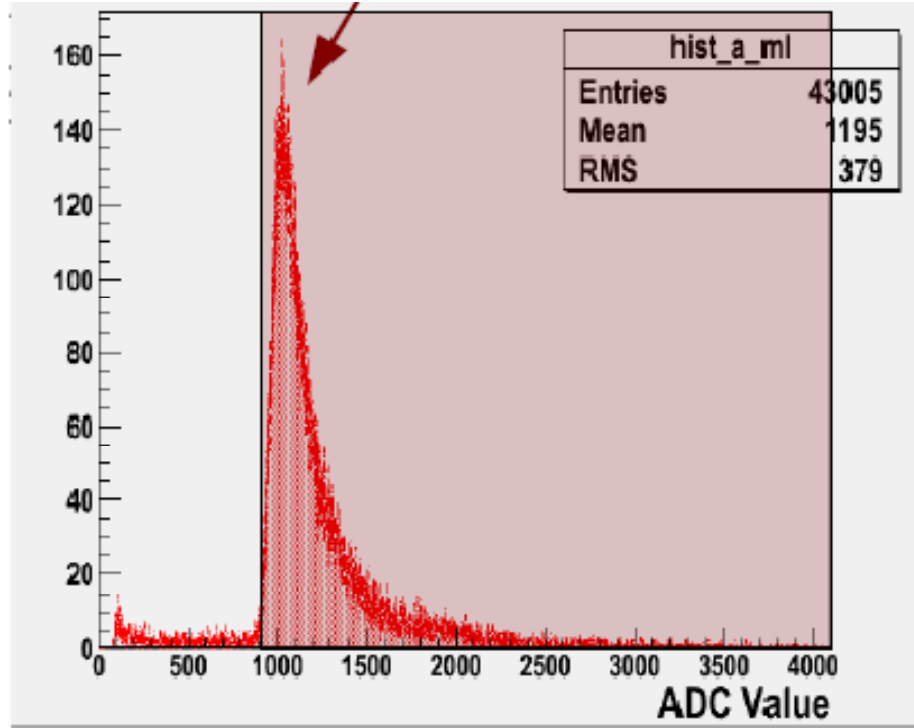
Figure 27: ADC cut (red).

Time-Walk Corrections

The greatest correctable source of smearing in our time resolution measurements comes from time walk. The symmetry of the PMTs used in the three-bar-method constantly ensures the rise time for each signal is the same, while the amplitude can clearly differ for varying positions. The leading-edge discriminator threshold is fixed, so there would be a delay on the TDC due to the different amplitudes, as seen in Figure 28. Correcting this time walk involves a parameterized correction to each TDC value including the reference, which in the three-bar-method comes from the middle left PMT.

$$t_{corrected} = (TDC_i - \frac{\lambda_i}{\sqrt{ADC_i}}) - (TDC_{ref} - \frac{\lambda_{ref}}{\sqrt{ADC_{ref}}})$$
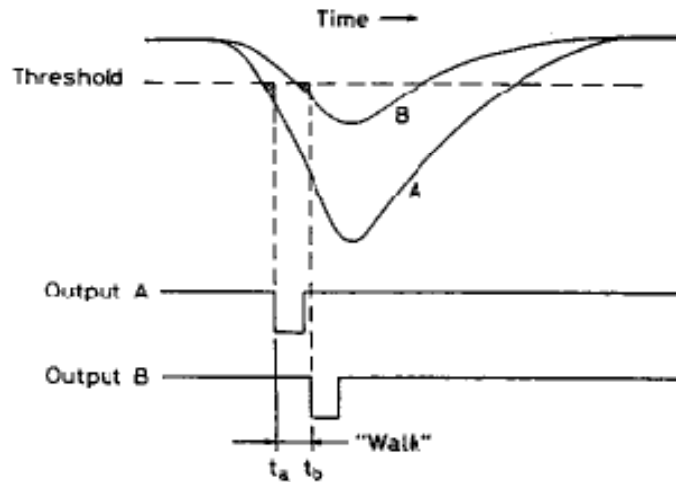
Figure 28: Time walk[20].

A program runs through a range of parameters to find the corresponding

minimum σ for the corrected TDC value distribution. The values that give the minimum

time resolution are then used for the correction. This minimum is only valid in the

region defined by the TDC cut, however. This process for time-walk corrections must be

automated for the full length of the counter.

---

[20] Signal A and B will arrive at the TDC at different times due to the difference in their respective
amplitudes. This time difference is referred to as "time walk".
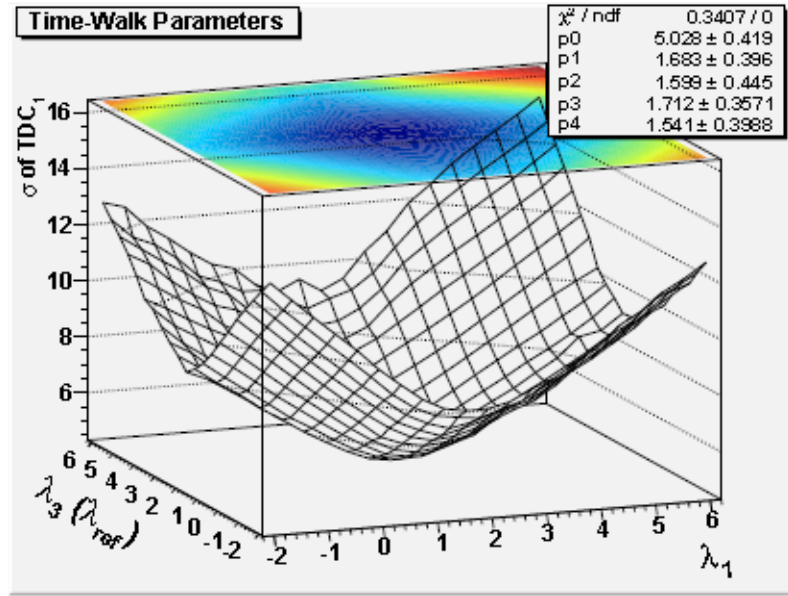
Figure 29: 3-D histogram of the time walk parameterizations[21].

Following the time-walk parameterization, the final time resolution at varying

positions based on the TDC difference cuts is calculated. Current results show an

average position-dependent time resolution of 39ps, with only slight variations towards

the end of the scintillator.

---

[21] The minimum can be found through careful analysis of the colored region of the histogram.
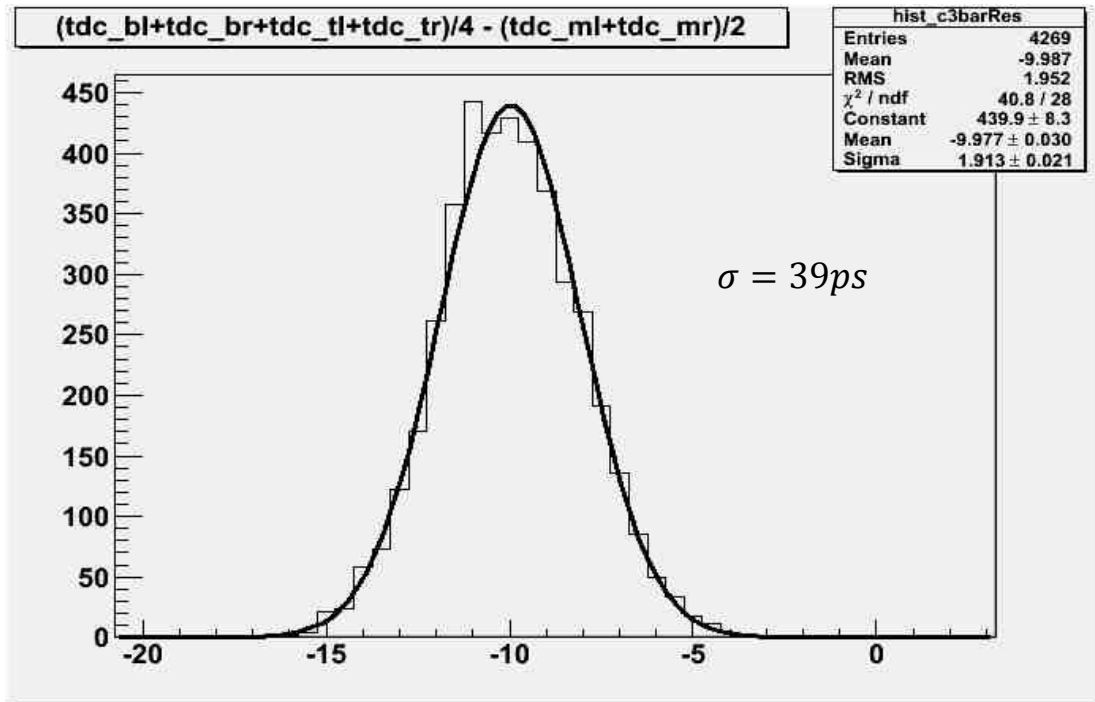
Figure 30: Time resolution[22] with no magnetic field.

Time-Resolution Measurements in a Magnetic Field

During a recent CLAS collaboration meeting, the question was raised as to whether or not small magnetic field inside the detector would not only influence the integrated analog signal from the PMTs, but even more so the time resolution. No effect was expected, however, because the shape of the analog signal did not appear to change under varying magnetic fields. To analyze this proposed phenomenon, the Helmholtz Coil is placed around one end of the three-bar-method apparatus. The magnetic field is set to 20 G first for a transverse field and then 10 G for an axial field.

---

[22] A Gauss fit provides the standard deviation, allowing for easy calculation of the time resolution. Sigma is multiplied by 25 (the bin width in ps) and then $\sqrt{2/3}$ from the calculation of the time resolution derived previously. The uncertainty in the Gauss fit leads to an uncertainty of 0.43ps.

Time-resolution measurements of 41 and 38ps in Figures 31 and 32 respectively are within the uncertainty of the time resolution measured without a magnetic field.
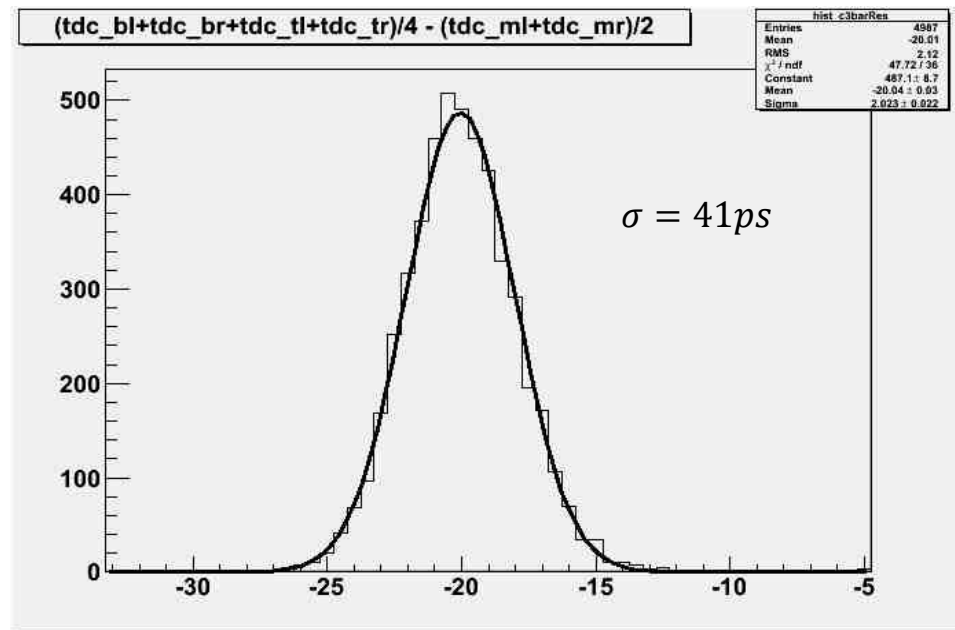

Figure 31: Time resolution with a 20 G transverse field.
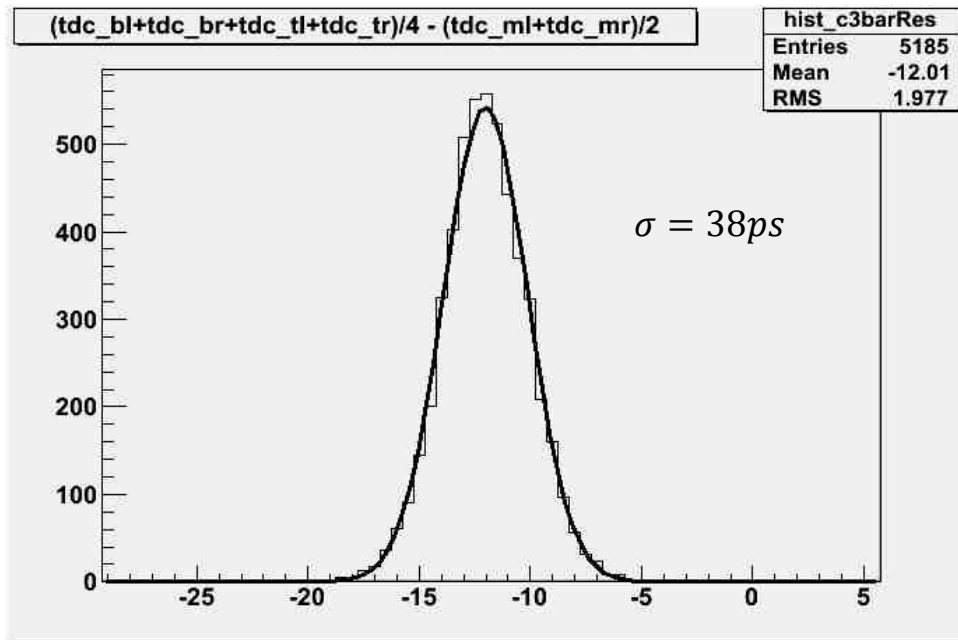
Figure 32: Time resolution with a 10 G axial field.

Conclusion

The magnetic field created by the toroidal magnet in the CLAS-12 detector has the possibility of detrimentally affecting the TOF12 time resolution. The qualitative analysis of the PMT pulse shape in a magnetic field led to an examination of the amplitude reduction as a function of the field's strength and orientation. The transverse and axial field measurements show the importance of mu-metal shielding as well as the range of its effectiveness. The axial fields do not reduce the ADC distribution dramatically until around 10 G, while the transverse fields require mu-metal shielding in the PMTs. Additional mu-metal shielding preserves the ADC distribution for transverse fields above 25 G. Active shielding would provide the solution to large axial fields. Each PMT used in the counter construction must be properly inspected for the maximum and minimum orientations, as well as to ensure that the mu-metal shielding provided by the company is adequate. The magnetic fields impact the time-resolution measurements significantly less than the integrated PMT signal.

Bibliography

Armstrong, & Smith. (1991). *CLAS-NOTE-91-018: Magnetic Shielding of Photomultiplier Tubes in the CLAS TOF.*

(2008). *CLAS12 Technical Design Report v5.0.*

Gothe, Phelps, Steinman, & Tian. (2009). *CLAS12 Time-of-Flight at USC: A Comprehensive Update.* Columbia: University of South Carolina.

Graham, L. (2008). *The Time of Flight Upgrade for CLAS at 12GeV.* Columbia: University of South Carolina.

Leo, W. (1987). *Techniques for Nuclear and Particle Physics Experiments.* Berlin: Srping-Verlag.